https://doi.org/10.20965/jdr.2020.p0765

Paper:

Full-Scale Experiment of Earthquake Resistant Embankment Using Flexible Container Bag

Hiroshi Nakazawa[*1,†], Yohsuke Kawamata[*2], Satoru Shibuya[*3], Shoji Kato[*3], Kyung-Beom Jeong[*3], Jemin Baek[*3], Tara Nidhi Lohani[*3], Akihira Morita[*4], Osamu Takemoto[*4], and Yoshitaka Moriguchi[*4]

[*1]Earthquake Disaster Mitigation Research Division, National Research Institute for Earth Science and Disaster Resilience (NIED)
3-1 Tennodai, Tsukuba, Ibaraki 305-0006, Japan
[†]Corresponding author, E-mail: nakazawa@bosai.go.jp
[*2]National Research Institute for Earth Science and Disaster Resilience (NIED), Hyogo, Japan
[*3]Kobe University, Hyogo, Japan
[*4]Hyogo Prefecture, Hyogo, Japan
[Received April 6, 2020; accepted June 15, 2020]

There exists many road embankments in Japan which are not earthquake resistant. For example, a road embankment collapsed at Okuradani IC in Hyogo Prefecture during the Great Hanshin-Awaji Earthquake of 1995. In 2009, a road embankment along the Tomei Expressway collapsed during an earthquake with epicenter in Suruga Bay. Road failure makes relief activity and transportation of goods difficult, causing social damage. Furthermore, recovery of damaged embankments takes much time and cost. Accordingly, it is important to conduct research on methods of construction which would help build embankments inexpensively and swiftly. Against this background, a full-scale experiment was conducted at E-Defense to confirm the validity of a method of construction that uses flexible container bag to pack soil for quick embankment recovery. Generally, flexible container bags are easy to handle, and ensure and maintain the earthquake resistance performance of embankments after the completion of recovery work, taking the longer life time of the reinforced structure into consideration. In the experiment, two kinds of reinforced structures with flexible container bags stacked differently were placed at either toe of the slope of an embankment of height 4 m, and shake tests were performed three times to compare the effectiveness of both reinforced structures. For both kinds of structures, the flexible container bags were stacked in two tiers and compressed from top and bottom using compression plates to make the structures rigid. One of the structures was one-tier type where the flexible container bags were stacked in series and the other was two-tier type where the flexible container bags were stacked along the side of the embankment. In the case with the target acceleration of sine wave of 376 Gal, crack occurred on the reinforced structure of one-tier type, but the embankment collapsed a little near the top of the slope. There was little displacement in both reinforced structures, hence, it is judged that the deformation would not impair the functionality of the road. As for the seismic performance, it can be said that the two-tier type would be slightly superior to one-tier type, however, this assumption cannot be evaluated decisively under the present circumstances. For practical use in future, form, size, workability, and economy of embankment should be examined for designing and construction which takes the specification of the structure into consideration.

Keywords: road embankment, flexible container bag, earthquake resistance, full-scale model, shake table test

1. Introduction

Many housing land and road embankments have suffered damage during earthquakes. Especially in the case of road embankments, the social and economic impact of the damage is significant, as the embankments temporarily fail to function as a linear structure. In Japan, many road and housing land embankments have either insufficient earthquake resistance or were constructed according to the previous earthquake resistant design code and have not been examined to confirm whether they meet the current earthquake resistant design code and performance requirements. For example, a road embankment collapsed completely at Okuradani IC in Hyogo Prefecture during the Great Hanshin-Awaji Earthquake of 1995 [1], and in 2009, a road embankment along the Tomei Expressway collapsed due to an earthquake with epicenter in Suruga Bay, rendering the major one of Japan's most major highways impassable [2]. Road failure makes relief activity and transportation of goods difficult, causing more social damage. Furthermore, restoring the damaged embankments takes much time and cost. Accordingly, it poses a major challenge in the earthquake proofing of social infrastructure which is a part of the research and develop-

ment centered on finding methods to build embankments inexpensively and swiftly [3]. Against this background, the Japanese Geotechnical Society advocates the advancement of "the development of the technology to judge the dangerous spots of the road embankments which are massive stock in Japan swiftly, inexpensively and precisely and the development of the method of reinforcement construction practicable effectively and economically" [4]. As a step toward the implementation of this proposal, two full-scale experiments were conducted in the fiscal year 2016–2017 at the Large Earthquake Simulator with a 1D shake table operated by the National Research Institute for Earth Science and Disaster Resilience (NIED). Then, at the 3D full-scale earthquake testing facility commonly referred to as "E-Defense" similarly operated by the NIED, another full-scale experiment was carried out in November 2019.

In these experiments, proposals were made to improve the earthquake resistance performance of embankments by using flexible container bags which are easy to handle and also minimize the scale of damage. These proposals aimed at both swift embankment recovery and finding earthquake resistance measures that will ensure longlife of the infrastructure. In this study, however, first a prediction analysis is conducted using an embankment model and then a full-scale experiment was carried out at E-Defense to measure the dynamic behavior and residual deformation of the embankment.

For this purpose, two different types of reinforced structures are installed by stacking flexible container bags differently at either toe of the slope of an embankment of height 4 m and their effectiveness was compared by conducting four times shaking tests. For both types of reinforced structures, the flexible container bags were stacked in two tiers and were compressed from top and bottom using compression plates to make the structures rigid. One of the structures is one-tier type where the flexible container bags are stacked in series and the other is two-tier type where the flexible container bags are stacked along the slope of the embankment. In case of a target acceleration with sine wave of 450 Gal as a shaking condition, a crack occurred in the reinforced structure of one-tier type, and the embankment collapsed a little near the top of the slope. For both types of reinforced structures, there was little displacement; therefore, it is judged that the residual deformation would not impair the functionality of the road.

As for the full-scale experiment at E-Defense, the number of cases are limited because of the experiment's scale and the experiment was conducted only once. Therefore, the cases without reinforcement measures could not be verified. However, based on the pre-analysis, the comparison of the deformation mode and the characteristics of acceleration response at the top of the slope suggested that in the cases without resistance measures, the embankment as a whole deforms, while in the cases with measures, the deformation was more remarkable in the upper part of the embankment than in the flexible container bags. As for the seismic performance of the reinforced structures, it can be said that the two-tier type would be slightly superior to one-tier type, however, it cannot be evaluated decisively under the present circumstances. In this paper, examples of road embankment damage were introduced and the results of the numerical analysis that was conducted on the basis of the results of the full-scale experiment and the analysis model used in the pre-analysis were discussed.

2. Examples of Damage and Previous Experiments

Even if only a part of road embankment collapses, the social and economic damage is significant since the road embankment's function as a linear structure fails. In this chapter, first, the actual examples of damage are introduced, followed by a summary of previous studies on embankment recovery and countermeasure construction. The next chapter then focuses on the full-scale experiment conducted as part of this study.

2.1. Examples of Damage Caused by Earthquakes

As for the large-scale damage caused by earthquakes in the past, a road embankment collapsed at Okuradani IC in Kobe City, Hyogo Prefecture and the housing land embankments in Yurigaoka, Nishinomiya City, and Ashiya City collapsed during the Great Hanshin-Awaji Earthquake of 1995 [1]. Then, there was a large-scale collapse along the Noto Toll Road during the Noto Hanto Earthquake in 2007, and in 2009, a road embankment along the Tomei Expressway in Makinohara, Shizuoka Prefecture collapsed during an earthquake with epicenter in Suruga Bay [2]. A brief description of each of these three incidents follows next.

2.1.1. Damage Caused at Okuradani IC by the Great Hanshin-Awaji Earthquake

The Great Hanshin-Awaji Earthquake struck the southern part of Hyogo on January 17, 1995, resulting in the collapse of an embankment of height 15 m near Okuradani IC along the Daini-Shinmei Road as shown in **Fig. 1**. According to the investigation report on the Great Hanshin-Awaji Earthquake [1], this road embankment was constructed on a site where a pond had once existed, and the foundation ground was soft with the N value being less than 5 up to 5 m in depth. As to the failure mechanism, it is estimated that the swelling of concrete block retaining wall caused by lateral deformation and ground surface settlement, and numerous cracks in the embankment triggered the collapse. Additionally, it is pointed out that the large amount of water leaked because of a rupture in a water pipe buried in the embankment contributed to the collapse.

Fig. 1. Damage situation at Okuradani IC [1].

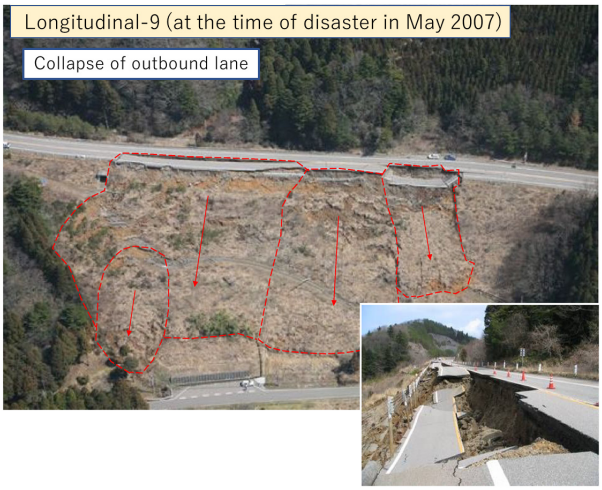

Fig. 2. Damage situation along the Noto Toll Road [5].

2.1.2. Damage Caused Along the Noto Toll Road by the Noto Hanto Earthquake in 2007

The Noto Hanto Earthquake in 2007 caused large-scale damage along the Noto Toll Road [5], following which a detailed survey was carried out to understand the tendencies of road embankment damage. The factors leading to the large-scale collapse (as shown in **Fig. 2**) are as follows: construction of high embankments in the valleys; the valleys acted as catchment areas for surface water and groundwater from hinterland and surrounding areas; at about 70% of the collapse sites, the collapsed sediment changed into mud that flows down to the lower part of a slope; performing soil boring tests, etc. It is also found out that the former geographical features remained as they were and there existed slip surface near the undersurface of embankment. These factors suggest that the shear strength of the embankment material with high moisture content rate at the top of the slope was lowered by the seismic motion, which led to collapse.

Fig. 3. Damaged lane of Tomei Expressway in Makinohara District [2].

2.1.3. Damage Caused at Makinohara District, Shizuoka Prefecture Along the Tomei Expressway

An embankment slope near Makinohara Service Area of the Tomei Expressway collapsed during a 2009 earthquake with epicenter in Suruga Bay. "The Committee on Earthquake Damage in Makinohara District of the Tomei Expressway" reported on the cause of the collapse [6]. According to the report, there was slight damage in districts other than Makinohara and the damaged infrastructure was restored with relatively easy repairs. However, in case of Makinohara as shown in **Fig. 3**, a 40 m long portion of the embankment slope of the Expressway's main lane collapsed. The above-mentioned committee was of the opinion that the slope surface collapsed because of the reduced shear strength and permeability of the structure. This was caused by the weathering of mudstone in the lower part of embankment over many years, which resulted in bad drainage and rise of groundwater because of this embankment's construction in the catchment area. Such conditions along with the embankment's inferior earthquake resistance triggered a sliding failure in the lower part of the embankment that gradually advanced to the upper part and finally reached the driving lane of the Expressway.

2.2. Restoration of Embankment Along the Tomei Expressway

In this section, emergency restoration of the damaged road embankment of the Tomei Expressway mentioned earlier is described. First, aiming to not add to the sediment runoff at the failure site, H-section steel columns were erected at the toe of the slope; large flexible container bags were placed and the upper part of the embankment was treated for cement stabilization to reduce the amount of sediment. Furthermore, a protective concrete layer was placed at the toe of the slope and large styrofoam blocks, which were lighter than sediments in

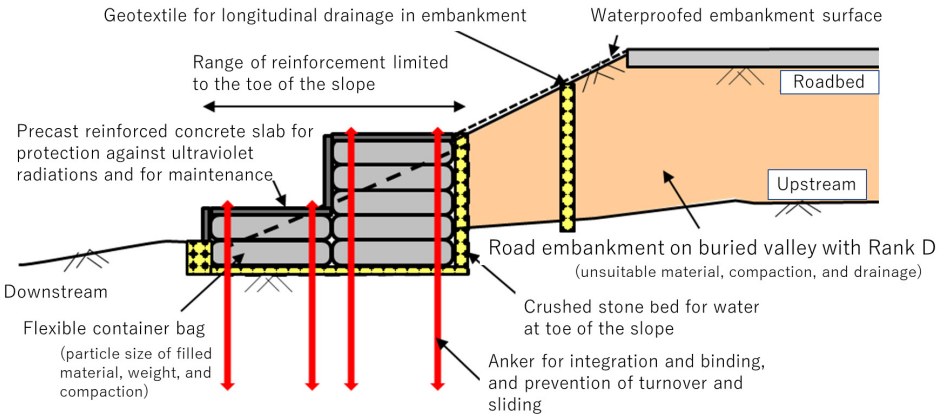

Fig. 4. Method of construction for restoration of embankment using flexible container bag.

weight, were laid to reduce the weight of embankment. The restoration work was carried out night and day so that after the occurrence of the earthquake at 5:07 am on August 11, the roadblocks in the outbound and inbound lanes were removed at 24 o'clock on August 12 and August 15, respectively. However, complete restoration took more time.

2.3. Previous Experiments

As is evident from the above examples of damage, it is important to develop a method of construction which would provide high earthquake resistance during emergency restoration, assure the safety of the process until complete restoration, and is also efficient in terms of total cost. Shibuya et al. [7] proposed using flexible container bags as an alternative method of construction as shown in **Fig. 4**. In this method of construction, the land surrounding the toe of the slope of an embankment is excavated, the excavated soil is tightly packed into the pillow-shaped flexible container bags, and the flexible container bags are then stacked and binded with the bedrock using ankers. To maintain the integration of the flexible container bag for a long time, the important points that need consideration are the size of the flexible container bag, deformation and strength characteristics of the material to be filled in the flexible container bags, compaction, and the technique of using the ankers (if necessary).

To evaluate the earthquake resistance of the flexible container bag structure, a small shake table test was performed under the conditions where the horizontal load corresponding to the lateral earth pressure of embankment was applied to the flexible container bags loaded with prestress [8].

First, the shake table test was conducted on an embankment with no reinforcement measure (Case 1) and then on an embankment reinforced with the flexible container bag structures (Case 2) using the full-scale model shown in **Fig. 5** [9]. For this experiment, the loading frequency in the direction of embankment section was regulated as $f = 2$ Hz and the amplitude of sine wave of 40 waves was adjusted to 100 Gal, 250 Gal, and 750 Gal until the

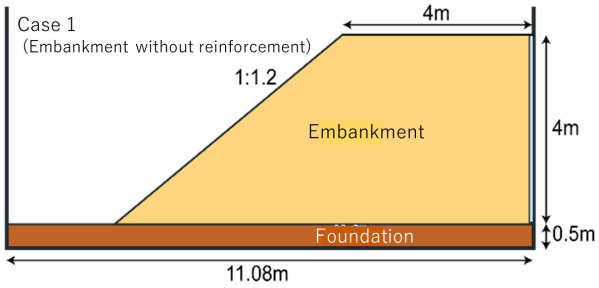

(a) Embankment without measure (Case 1)

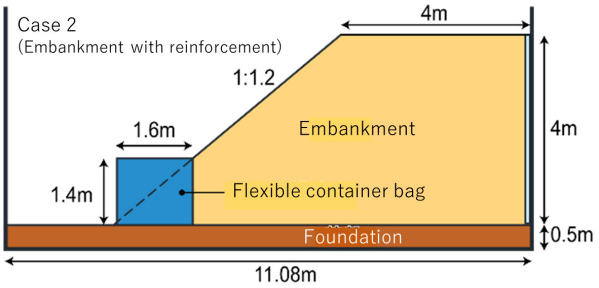

(b) Embankment with measure (Case 2)

Fig. 5. Section of previous full-scale experiment.

collapse of the embankment was confirmed. From the results of 3D territorial laser measurement before and after the experiment [10], the effectiveness of the reinforced structure was confirmed (see **Fig. 6**), as the sliding surface generated at a point higher than the reinforced area (height of 1.4 m above the foundation) in Case 2 so that the scale of the sliding sediment became smaller.

3. Full-Scale Experiment at E-Defense

In this chapter, the full-scale experiment conducted at E-Defense is described. Since the number of cases was limited due to the scale of the experiment, the experiment was conducted only once. Furthermore, referring to the results of the experiment mentioned in Section 2.3,

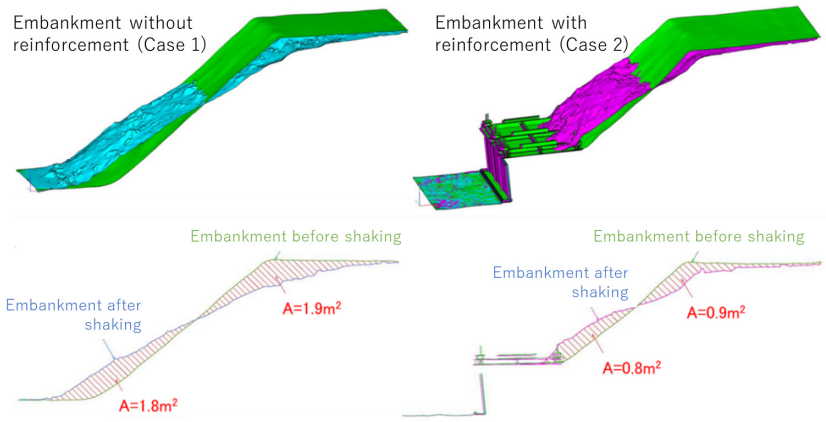

Fig. 6. Results of 3D territorial laser measurement before and after experiment.

the effectiveness of using flexible container bags at the toe of the slope for reinforcement was confirmed. Therefore, in this experiment, the effectiveness was not verified using the embankment without measure case, instead two types of reinforced structures with the flexible container bags stacked differently on the same embankment are compared for effectiveness. In the next sections, the experiment is described in terms of the specification of the model.

3.1. Concept of the Experiment

Before describing the experiment, its concept is explained based on the discussion in Section 2.

Three examples of road embankment damage caused by earthquakes were already mentioned in Section 2. In the case of great collapse caused at Okuradani IC, microtopography such as high embankment on soft ground was a significant factor against the damage, whereas the natural ground materials at the toe of embankment's slope were the main factor on the damage caused along the Noto Toll Road and the Tomei Expressway. Regarding the restoration after the damage, the case of Tomei Expressway showed that temporary restoration was possible at the earliest, but it took much more time to complete the restoration process. Taking these examples and the experiment discussed in Section 2.3 into consideration, reinforcement using flexible container bag and ankers as a measure against soft ground is proposed and an experiment is conducted to verify the effectiveness of the reinforced structures.

As mentioned above, the objective of this study is to find an inexpensive and swift method of construction for earthquake resistant reinforcement of road embankments that will also ensure longlife of such reinforced structures. However, as the stock of compression plate for the flexible container bags and the workability of the ankers and flexible container bags determined depending on the condition of the foundation can influence the actual cost, it is still not clear whether the objective of this study could be achieved if the number of constructed structures at the sites dose not increase. Accordingly, taking the implementation at the sites into consideration, different types of flexible container bags were evaluated in this experiment. The experiment was planned in such a way so as to obtain the basic data to identify a favorable method that will not only temporarily restore the embankments after damage but will also lead to better workability and longlife of the reinforced structure by improving its earthquake resistance and reducing the construction period.

Fig. 7. Overall view of soil container for full-scale experiment.

3.2. Shake Table and Soil Container

The experiment is conducted using the shake table at E-Defense. The specifications of the shake table are: it supports the maximum loading capacity of 1,200 t, maximum acceleration with the maximum weight loaded is 900 cm/s^2 in the lateral direction and 1,500 cm/s^2 in the vertical direction, and the maximum displacement of $\pm$100 cm in the lateral direction and $\pm$50 cm in the vertical direction. Using this shake table, it is possible to simulate the earthquake collapse behavior of an embankment model of height 4 m.

On this shake table, a rectangular parallelepiped steel soil container was set as shown in **Fig. 7** and a model using the flexible container bags was built inside the soil

Table 1. Physical and dynamic characteristics of embankment material.

Density of soil particles	ρ_s	(g/cm^3)	2.615
Maximum particle size	D_{max}	(mm)	75.0
Fine content (<0.075 mm)	F_c	(%)	11.4
Optimum water content	w_{opt}	(%)	10.4
Maximum dry density	ρ_{dmax}	(g/cm^3)	1.998
Cohesion	c_d	(kN/m^2)	14.7
Angle of shear resistance	ϕ_d	(°)	36.1
Initial modulus of rigidity	G_o	(MN/m^2)	30.6
Maximum damping constant	h_{max}	(%)	14.2

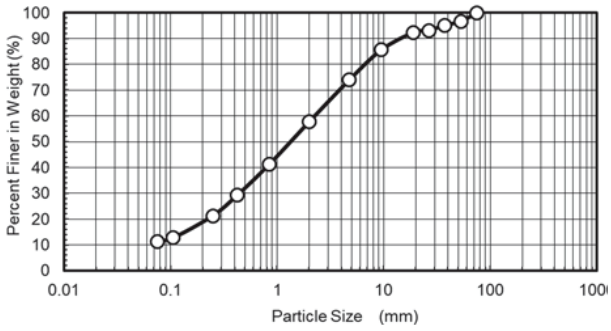

Fig. 8. Grain size distribution curve of embankment material.

container. Its dimensions are: width = 4.0 m, height = 4.5 m, and length = 16.0 m; thus, it was possible to build a full-scale embankment in the soil container.

3.3. Overview of Embankment Model

In the soil container shown in **Fig. 7**, the model was so built that the two types of reinforced structures with flexible container bags stacked differently are constructed at either toe of the slope of the embankment with height 4 m. The ground material used for the embankment, construction of the reinforced structure using sandbags, and its cross section are explained in the next sections.

3.3.1. Ground Material

The physical and dynamic characteristics of the embankment material used for the experiment are listed in **Table 1** and its grain size distribution curve is shown in **Fig. 8**. The ground material consists of gravelly sand with fine (SF-G) with the maximum particle size of 9.5 mm and the maximum dry density of 2.15 g/cm^3. The internal friction angle (ϕ') of the ground material is around 52° compared to 30° to 35° which is generally regarded as good quality, indicating that the ground material is of superior quality. The dynamic deformation characteristics of the embankment material are shown in **Fig. 9** and are used for the prior numerical analysis as a modified RO model [11].

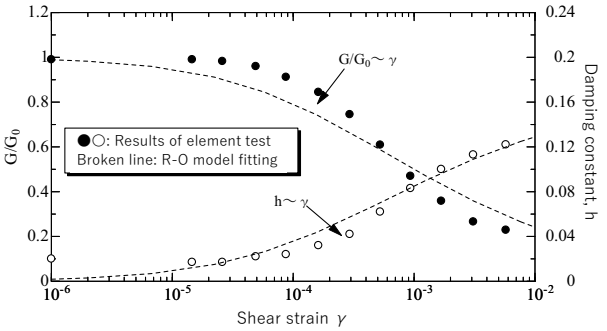

Fig. 9. Dynamic deformation characteristics of embankment material.

3.3.2. Preparation of Embankment and Finished Shape

Figure 10 shows the outline and cross section of the model, which was so prepared that the two types of reinforced structures with flexible container bags stacked differently were constructed at either toe of the embankment slope. For both types of reinforced structures, the flexible container bags were stacked in two tiers and were compressed from top and bottom using compression plates to make the structures rigid. One of the structures is one-tier type where the flexible container bags are stacked in series and the other is two-tier type where the flexible container bags are stacked along the side of the embankment.

To prepare the embankment, it was first divided into 15 layers in the soil container with the help of a mini backhoe and the ground material was placed and leveled. Then, rolling compaction was carried out 8 times using a hand roller so that the degree of compaction D_c reached around 90%. To control the soil density of each layer after rolling compaction, soil densities were checked using the RI instrument (JGS 1614-1995) and conducting sand replacement method (JIS A 1214). Average water content w_c in the finished shape is 6.3% by RI method and 6.7% by sand replacement method. The average degree of compaction was measured 87.6% by RI method and 89.0% by sand replacement method. Finally, after the completion of the spreading of soil and rolling compaction up to the crest, the crest was paved with asphalt and the embankment is prepared.

Although the height of the model was 4.0 m according to the original plan, the final finished shape was short of 0.1 m so as to secure the slope gradient of 1 : 1.5 and the width of crest of 3.0 m.

3.3.3. Construction of Flexible Container Bag

Figure 11 shows what the flexible container bags look like during the construction. The actual construction of the reinforced structure was carried out at the designated place before preparation of the embankment as described in Section 3.2.1. The construction procedure is as follows: 1) setting the foundation and ankers for fixture of the flexible container bag, 2) preparing the foundation ground for the embankment and the embankment itself,

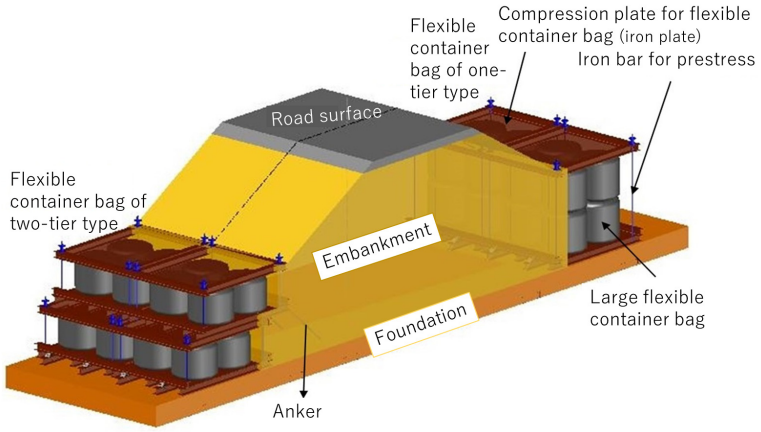

(a) Outline of reinforcement

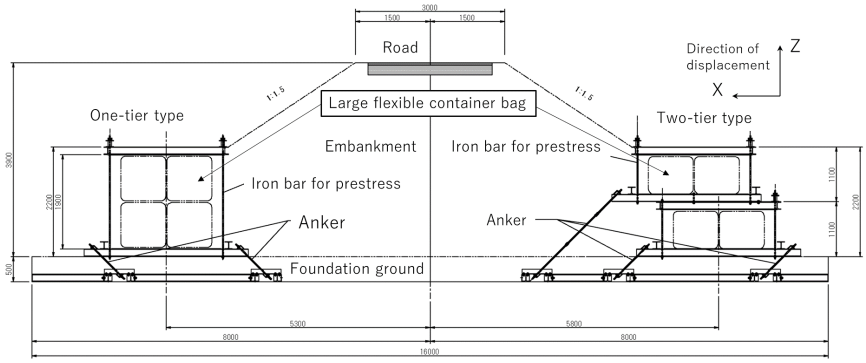

(b) Cross section of model

Fig. 10. Outline and cross section of model.

Fig. 11. Situation of flexible container bags.

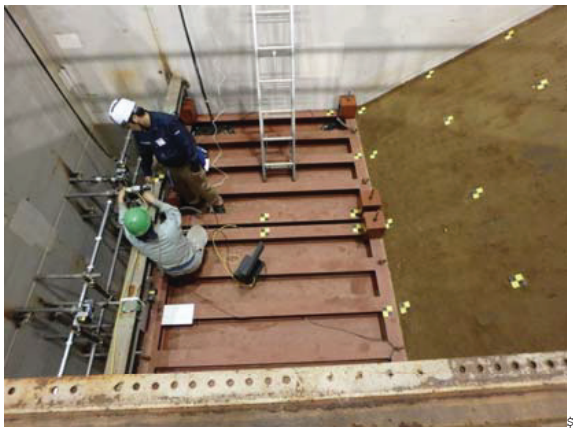

Fig. 12. Placement of the top frame of compression plate.

3) setting the bottom frame of compression plate, 4) placing the flexible container bags and the top frame of compression plate (**Fig. 12**), and 5) fixing both compression plates using bolts under the control of load and putting the flexible container bags under pressure. The prestress in step 5) was controlled with an anker axial tension of 100 kN/m^2. It is confirmed that after the relatively large reduction in prestress immediately after the loading, it finally converged to about 70 to 80%. However, the change in the volume of the flexible container bag with the prestress decreased and the creep characteristics were not measured quantitatively.

3.4. Conditions of Shaking and Measurement Plan

Table 2 shows the conditions of shaking. As for the shaking wave, the amplitude of the sine wave of 40 waves with $f = 5$ Hz was set as 100 Gal, 250 Gal, and 450 Gal, before a final shaking of 750 Gal was provided. While considering the conditions of shaking, a previous study was referred in which the experiment was conducted on a pond embankment of similar scale [12]. The maximum acceleration generated at the bottom of the soil container

Table 2. Conditions of shaking.

Case	Shaking wave	Target acceleration (Gal)	Response acceleration of shake table (Gal)
Case1	Sine wave, 5 Hz, shaking of 40 waves	100	125
Case2		250	245
Case3		450	376
Case4		750	660

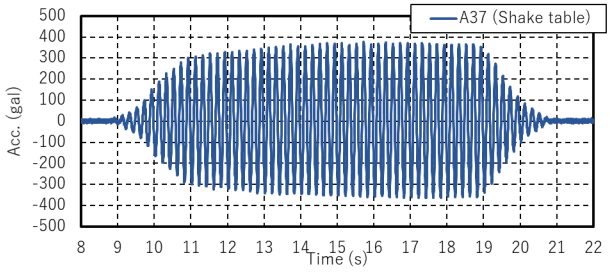

Fig. 13. Input wave (Case 3).

in each case was 125 Gal (Case 1), 245 Gal (Case 2), 376 Gal (Case 3), and 660 Gal (Case 4) which are determined as the experiment conditions. **Fig. 13** shows an example of a shaking wave.

Data measurement was carried out using 37 accelerometers for the model of embankment, flexible container bags, and shake table; 28 laser displacement sensors for the model of embankment and flexible container bags; 12 load cells for control of the prestress load of the flexible container bag; and 20 strain gauges for measurement of the anker axial tension. The yellow and black-colored targets for 3D dynamic measurement were arranged on the slopes of the embankment and the upper frames of compression plate to analyze the dynamic behaviors at the time of shaking. In addition, 3D territorial laser measurement is carried out before and after the shakings with amplitudes of 376 Gal and 660 Gal to analyze the residual deformation. As lots of data was collected using the sensors, only the results necessary for explanation are discussed in the next chapter.

4. Results of Experiment

As mentioned above, four cases were tested in the experiment. Of all the cases, Case 4 is tested with the intention to destroy the model and make some targets disappear due to the movement of sediment on the slope surface. As for the dynamic behavior, the results of the shaking experiment of Case 3 (376 Gal) and the response accelerations obtained from the numerical analysis are compared to confirm the reinforcement effectiveness of the flexible container bags. Furthermore, results of 3D territorial laser measurement before the experiment and after the Case 4 shaking (660 Gal) are compared to confirm the effectiveness of the reinforced structures based on the collapse form and residual deformation of the embankment.

4.1. Experiment Results

The results of response acceleration and response displacement at the representative spots are explained below.

4.1.1. Response Acceleration

Figure 14 shows the location map of the sensors. **Fig. 15** shows the time history of the results of measurement of the response acceleration at the toe of the slopes on the sides of one-tier and two-tier types (A26 and A28) in Case 3. Compared to the acceleration at the shake table (A37), an amplitude exceeding 4,000 Gal is recognized at the top of the slope corresponding to the input acceleration of 376 Gal. As for the response acceleration at the upper part of the flexible container bags (A32 and A35), there is a significant difference between one-tier and two-tier types and it is confirmed that the response acceleration of one-tier type exceeds 1,500 Gal and that of two-tier type marks 886 Gal. A possible reason behind such large amplitude of the response acceleration in the embankment could be that the predicted value of natural period of the model was about 6 Hz, while the preliminary value determined by the actual random wave was about 8 Hz, which was possible that the dynamic characteristics of the embankment was close to resonance due to damages with repeated shake tests. This possibility remains a conjecture as of now and should be examined further in detail.

4.1.2. Results of Measurement of 3D Dynamic Displacement Sensor

Figure 16 shows the layout drawing for shooting and the arrangement plan of targets. The camera was set at a depression angle of 70° to the direction of shaking, and the angle between the slope surface of embankment and the surface of imaging element of the camera was 36.1°. D_{yp} in **Fig. 16** indicates the vertical component of the gauge mark (P_{nm}). The high speed camera used for shooting had an earthquake resistant structure with an image resolution of $1,600 \times 1,200$ pixels and shooting speed of 1,000 frames per second. The position of the target and the displacements generated in the direction of shaking were traced and the vertical direction was summarized as time history.

Since some targets disappeared after the collapse of the surface layer of the slope of the embankment in Case 4, the dynamic behaviors were explained based on the results of Case 3 where the deformation of the embankment began and it can be analyzed how the embankment got deformed. **Fig. 17** shows the displacement at the top of the slope for one-tier and two-tier types and that in the upper part of the flexible container bags in Case 3. As to the displacement at the top of the slope, the horizontal displacement increased with the shaking, but the displacement in one-tier type was smaller than that in the two-tier type. As for the vertical displacement, in case of one-tier type, the displacement increased with the increase in horizontal displacement immediately after the shaking, while in two-tier type, there was a delay in the generation of vertical displacement. Focusing on the displacement in the

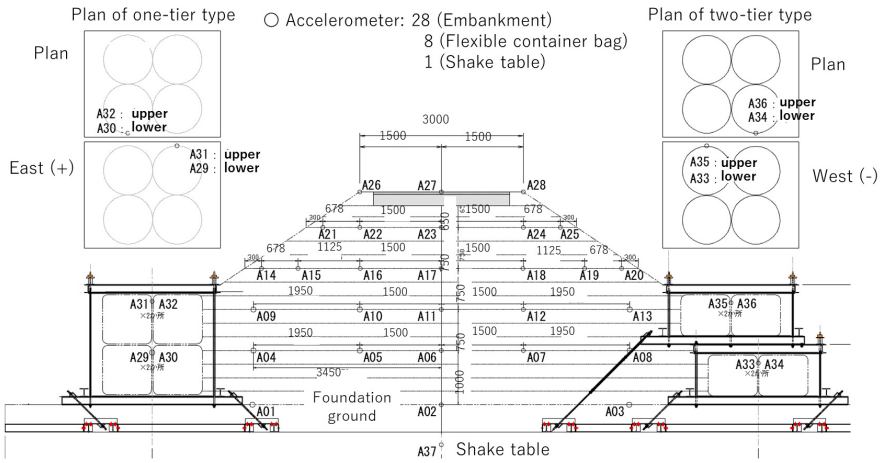

Fig. 14. Location map of sensors.

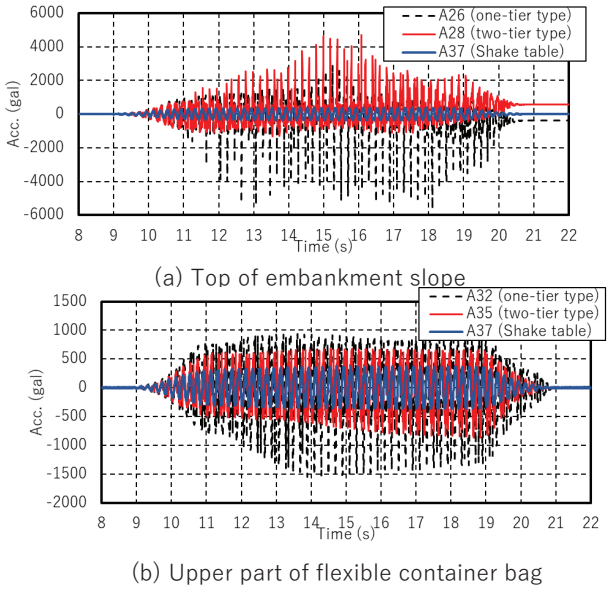

Fig. 15. Response acceleration at the top of the slope of embankment.

upper part of the flexible container bags, there is no significant difference in horizontal and vertical displacement between the two types of structures, and it is understood that a settlement in the vertical direction is remarkable compared with horizontal displacement.

Based on these findings from Case 3, any difference in the response acceleration and deformation characteristics of the embankment cannot be confirmed. As for the flexible container bags, it is characteristic that the response acceleration in one-tier type is distinguished. This might be because the one-tier type is structurally more unstable and the natural period of the flexible container bag could trigger resonance. However, it is surmised that at this stage it is not an external force which could lead to collapse of the embankment, so that no difference cannot be recognized in the deformation behaviors.

4.1.3. Analyzing Residual Deformation Using 3D Territorial Laser Measurement

Prior to the measurement, multiple targets were set as fixed points in the soil container to synthesize the data and the measurement is made, taking the constraint of the workplace into consideration. The distance is calculated by the time when the irradiated laser pulse is reflected by the object and returns. As the laser is continuously automatically irradiated while rotating, a large amount of point data can be obtained at one time. However, by using only one point, the distance from the measurement location can be obtained. If there is a blind spot, the shape of the embankment body cannot be expressed in 3D. Therefore, in this experiment, measurement was made from multiple random spots to convert the synthesized data into 3D as point group.

Figure 18 shows the contour figure of vertical change seen from above the embankment (the elevation after and before shaking) in Cases 3 and 4. In Case 3 shown in **Fig. 18(a)**, the crest part shows light blue over the entire surface and the settlement of about 6 cm can be seen. Both shoulders of slope are colored blue and the settlement corresponding to a collapse of about 12 cm is confirmed. On the other hand, both slope surfaces on the sides of one-tier and two-tier types are yellow and an uplift of about 6 cm can be seen there. **Fig. 19** shows the details from the deformation of the shoulder of the slope to the uplift of slope surface. It is thought that this was basically caused by the influence of the settlement of the embankment as a whole and its lateral swelling and additionally by the influence of covering of the collapsed sediment from the shoulders of slopes on the slope surfaces. For reference, the plane contour figure of Case 4 is shown in **Fig. 18(b)**. It can be seen that the scope of the deformation of the shoulder of slope enlarges, the slope surfaces uplift more, and the collapsed sediment is concentrated on the line between the flexible container bag of one-tier type and the embankment. Such situation is shown in **Fig. 20**.

Next, the deformation diagram on the centerline of the soil container in the direction of shaking in Cases 3 and

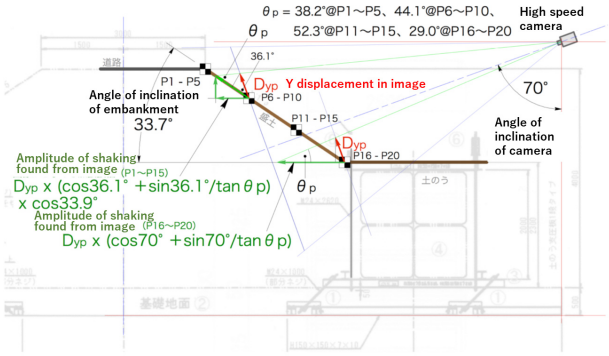

(a) Layout drawing for shooting

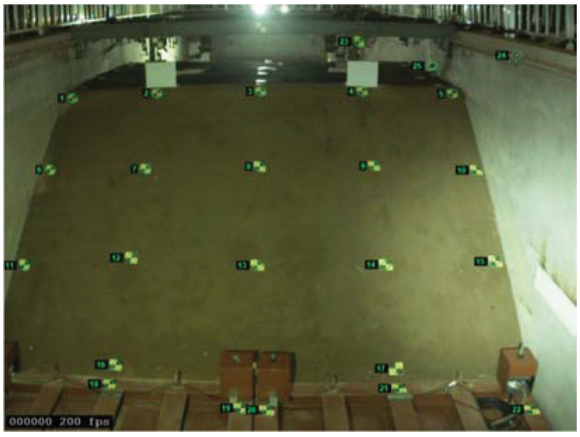

(b) Target arrangement (one-tier type)

(c) Target arrangement (two-tier type)

Fig. 16. Measurement of 3D dynamic displacement sensor.

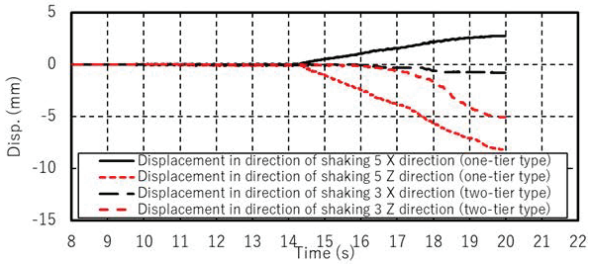

(a) Top of slope of embankment

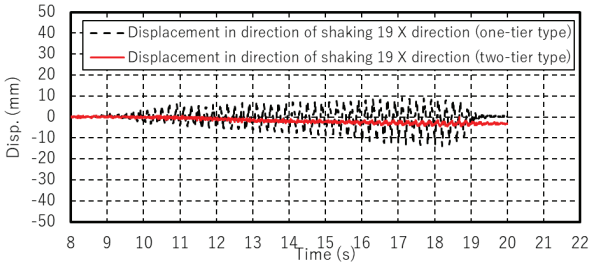

(b) Top frame of compression plate for flexible container bags (one-tier type)

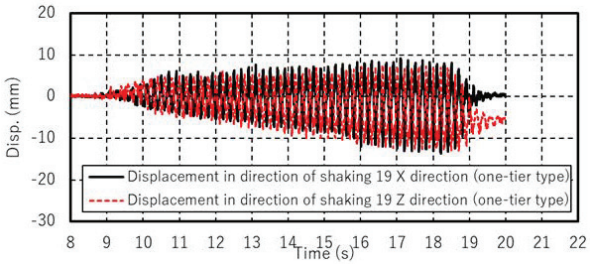

(c) Top frame of compression plate for flexible container bags (two-tier type)

Fig. 17. Results of measurement of 3D dynamic displacement sensor.

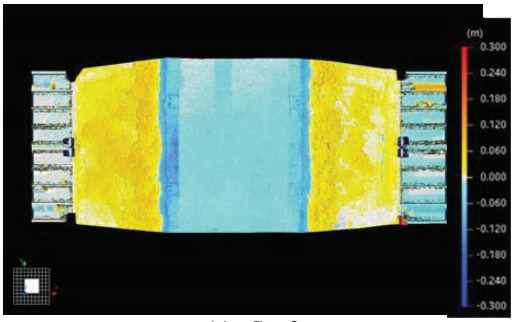

(a) Case3

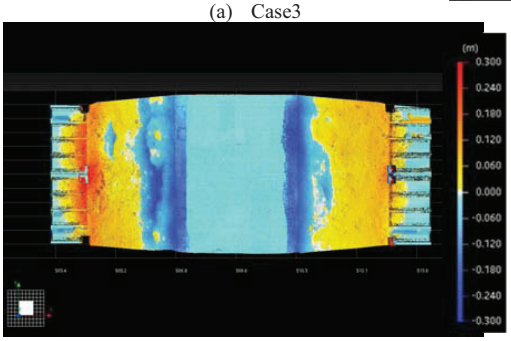

(b) Case4

Fig. 18. Results of 3D territorial laser measurement.

4 is shown in **Fig. 21**. From the results of the measurement after Case 4, the lateral displacement of the top frame of the compression plate for the flexible container bag of one-tier type was about 40 mm and that for two-tier type was about 50 mm. Though there is no direct comparison between the two because of how the flexible container bags were stacked, the lateral displacement in one-tier type was a little larger than that in two-tier type. As to the shoulder of the slope, the settlement in one-tier type was 186 mm and that in two-tier type was 178 mm, indicating tendencies opposite to that of the flexible container bags. As for displacement of the shoulder of the slope, similar to the explanation of dynamic behaviors, it

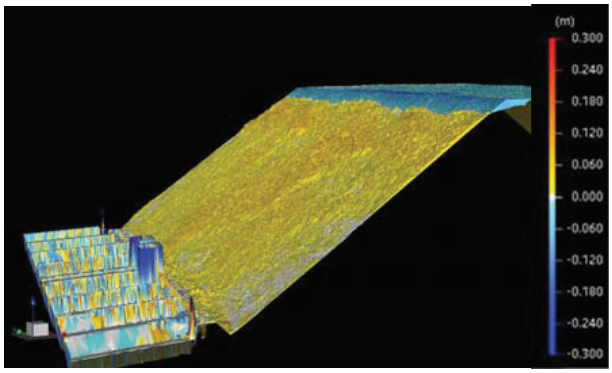

(a) One-tier type

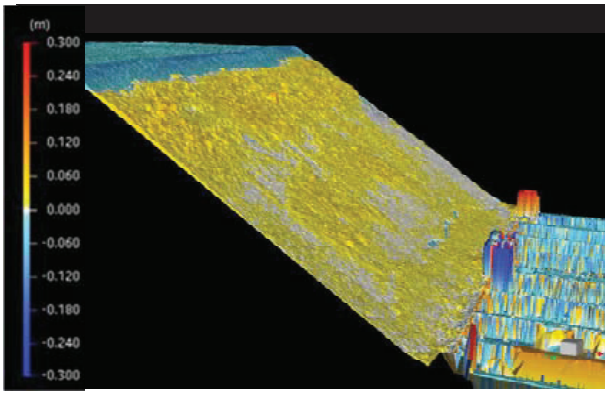

(b) Two-tier type

Fig. 19. Results of measurement of 3D dynamic displacement sensor.

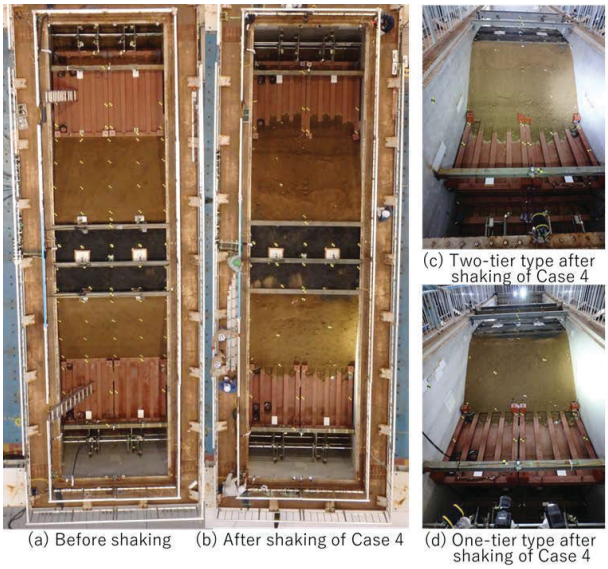

(a) Before shaking (b) After shaking of Case 4 (c) Two-tier type after shaking of Case 4 (d) One-tier type after shaking of Case 4

Fig. 20. Experiment situation.

is surmised that the residual deformation became larger in one-tier type than two-tier type because of the unstable flexible container bag structure and its resonance with the embankment under the condition of the destructive external force such as in Case 4. It could be said that in spite of a slight difference, two-tier type is superior in terms of functionality of road. However, judging from the results of this experiment, comparison with the characteristics of the seismic motion should be needed.

The abovementioned measurement results concerned the configuration of the embankment surface. Results of the handy dynamic cone penetration test [13], carried out both before and after the shaking, are shown in **Fig. 22** and the damage caused to the embankment can be confirmed. The survey locations were already shown in **Fig. 21**. As the asphalt pavement model imitating road is placed on the crest, the survey was conducted at the shoulder of the slope. The cone penetration resistance q_d shows the periodical peaks from the ground surface, irrespective of before or after the shaking and the type of flexible container bag structure. Such peaks indicate the rolling compactions during the construction. As the values of q_d was about 10 Mpa, both before and after the shaking, for both structure types and there was no significant difference in the tendencies, sliding surface cannot be estimated at the cone penetration points.

4.2. Evaluation by Numerical Analysis

This full-scale experiment focuses on embankment reinforcement by setting the flexible container bags at either toe of the slope; therefore, the earthquake resistance of the embankment without reinforcement is not evaluated at the same scale. Accordingly, a two-dimensional mesh for the experiment section shown in **Fig. 23** was generated and additionally, the mesh assuming the model without reinforcement was also done. The numerical analysis was conducted as the total stress analysis. As to the dynamic behavior during the shaking, the dynamic deformation characteristics shown in **Fig. 9** were used as the nonlinear hysteretic characteristics of the ground, joint element was set between flexible container bags, and the bottom was considered as bottom fixed boundary. Ground constants used for the analysis were shown in **Tables 3** and **4**.

4.2.1. Results of Analysis

As the condition of analysis, the input wave which was measured actually was used in each case shown in **Table 2**. **Fig. 24** shows the residual deformation diagrams of the model of flexible container bag and that of embankment without reinforcement under the condition of shaking in Cases 1 and 3 as the representative results of the analysis. The contour color indicates the lateral displacement. Since the deformation volume is small, the results of analysis are explained based on deformation mode only. In the case of embankment without reinforcement, the overall settlement occurs with the swelling of the slope surface. In the case of model with flexible container bag, the structure of one-tier type deforms and a swelling due to the large horizontal displacement of the slope on the same side is recognized. However, for two-tier type, there is no such displacement as one-tier type but the settlement becomes larger at the top of slope. This

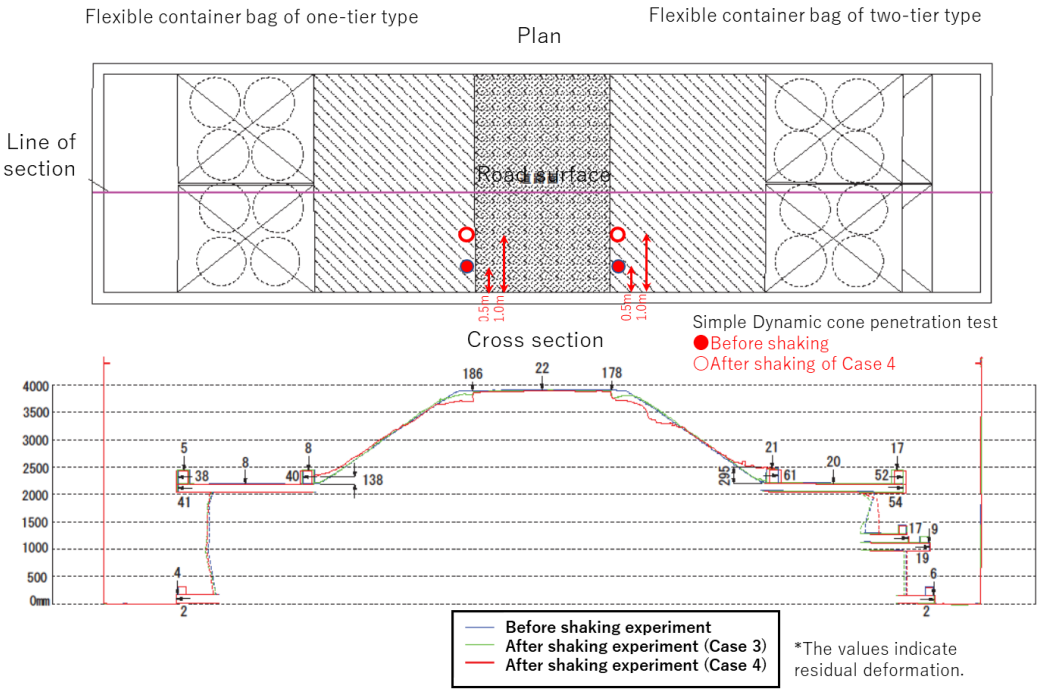

Fig. 21. Deformation diagram on centerline in direction of shaking.

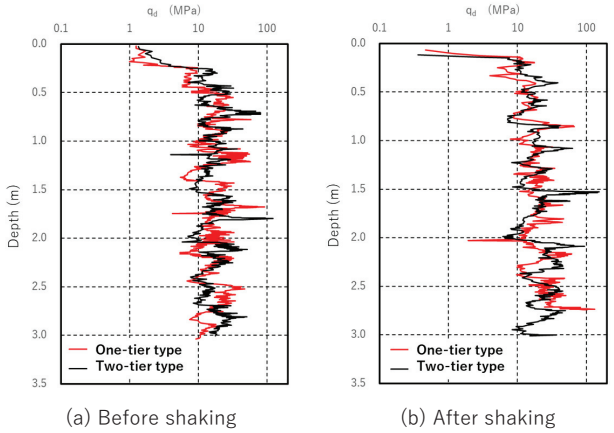

Fig. 22. Simple dynamic cone penetration test.

is thought to be caused by the fact that the flexible container bag of one-tier type is more vulnerable to deformation than that of two-tier type.

The distribution diagrams of the maximum horizontal acceleration in Cases 1 and 3 are shown in **Fig. 25**. Although the acceleration distribution generated in the embankment without reinforcement is a little complex, it can be seen how it amplifies upward laterally. In the case of model with flexible container bag, a large acceleration generates at the joint elements between the flexible container bags and the flexible container bags has a slightly rigid structure, therefore, this model shows a larger acceleration in the upper part of the flexible container bags compared to that in the embankment without reinforcement.

4.2.2. Characteristics of Amplification of Acceleration

The amplification rates at the shoulder of the slope and upper part of the flexible container bag structure based on the acceleration of the shake table, obtained from the results of the numerical analysis and full-scale experiment in this study are shown in **Table 5**. This summary indicates the results of Case 3. In both the numerical analysis and full-scale experiment, the amplification rates at the shoulder of the slope and upper part of flexible container bag are larger in one-tier type model. Furthermore, in the numerical analysis, the amplification rate in the embankment without reinforcement is a little less compared to that of both the reinforcement types of flexible container bag. This might have been caused by the fact that the level of the upper part of the flexible container bag becomes a virtual foundation surface and the height of the embankment becomes lower. Although the results obtained from the numerical analysis and the full-scale experiment show similar tendencies overall, there can be recognized prominent dissimilarities each other. The reason behind these differences could be found in the fact that the analysis model does not express the collapse and reflect the input parameters precisely. The resonance of the flexible container bag and the interpretation of the interaction between the embankment and the flexible container bag structure are one of the problems in the experiment. Accordingly, it remains a problem as to how to treat the joint element set in the analysis while considering the collapse phenomenon.

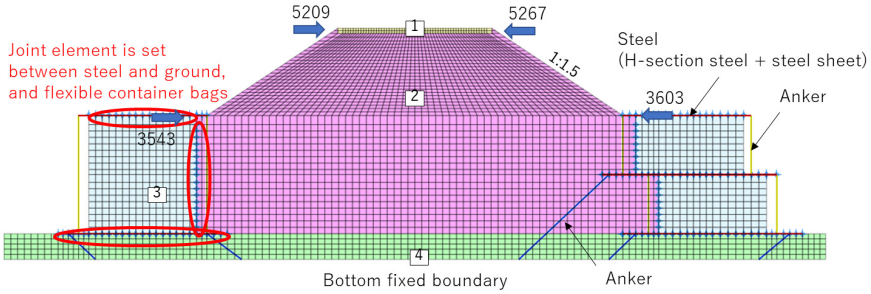

(a) Model for flexible container bag

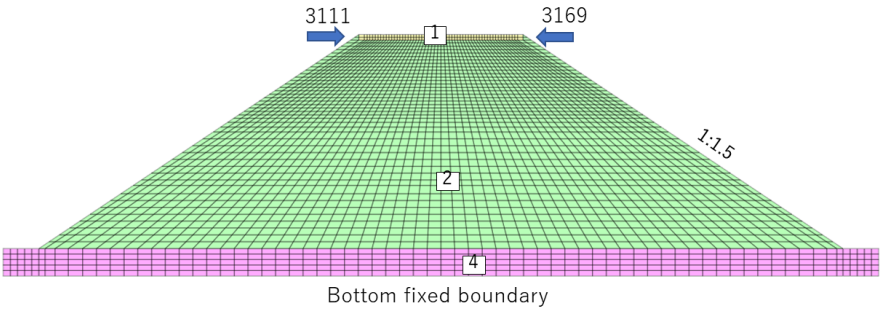

(b) Model for embankment without reinforcement

Fig. 23. Mesh diagram for numerical analysis.

Table 3. Ground constants for analysis.

Material number	Name	Poisson's ratio, ν	Weight of unit volume, γ (kN/m^3)	Elastic wave velocity, V_s (m/s)	Shear modulus, G (kN/m^2)	Young's modulus E (kN/m^2)	Width, h (m)	Standard strain, γ_r	Non-linear characteristics (Value at h_{max})	G	γ_r	Remarks
1	Paving	0.45	19.0	200	2476	7179	1.00	-	-	-	-	Standard confining pressure is assumed 0.1 kN/m^2 and modelled as elastic body
2	Embankment	0.45	19.0	126	30759	89201	1.00	1.00E-03	0.17	3107.1	1.010E-04	Standard confining pressure is assumed 98 kN/m^2
3	Flexible container bag	0.45	19.0	150	43593	126419	1.00	1.00E-03	0.17	-	1.010E-04	Dependence on confining pressure is not considered
4	Base ground	0.45	19.0	200	77498	224745	1.00	1.00E-03	0.17	7828.5	1.010E-04	Standard confining pressure is assumed 98 kN/m^2

Table 4. Material constants for analysis.

Name	Specification	Cross section (m^2)	Moment of inertia of area, I_z (m^4)	Moment of inertia of area, I_y(m^4)	Torsional moment, I_x(m^4)	Weight of unit volume, γ (kN/m^3)	Young's modulus, E (kN/m^2)
H-section steel	H150	0.003965000	1.6200E-05	5.6300E-06	1.6200E-05	77.0	2.0E+08
Steel plate	t=10 mm	0.010000000	8.3333E-08	8.3333E-08	8.3333E-08	77.0	2.0E+08
Anker (between flexible container bags)	ϕ24	0.000452389	1.6286E-08	1.6286E-08	3.2572E-08	77.0	2.0E+08
Anker (between flexible container bag and soil container)	ϕ24	0.000452389	1.6286E-08	1.6286E-08	3.2572E-08	77.0	2.0E+08

5. Conclusions

As complete restoration of the damaged embankments takes much time and cost, research is being conducted to develop methods of construction which would help build road embankments inexpensively and swiftly. To this end, a method of construction using flexible container bags which are easy to manage was proposed and a full-scale experiment was carried out to verify the effectiveness of this proposal.

In the experiment conducted at E-defense, the number of the cases was limited due to its scale and the experiment was conducted only once. Therefore, the flexible container bags of one-tier and two-tier types stacked differently at either toe of the slope of an embankment were prepared to compare and verify the effectiveness of the structures. The results of shaking experiment in Case 3 (376 Gal) show that the shoulder of the slope collapses a

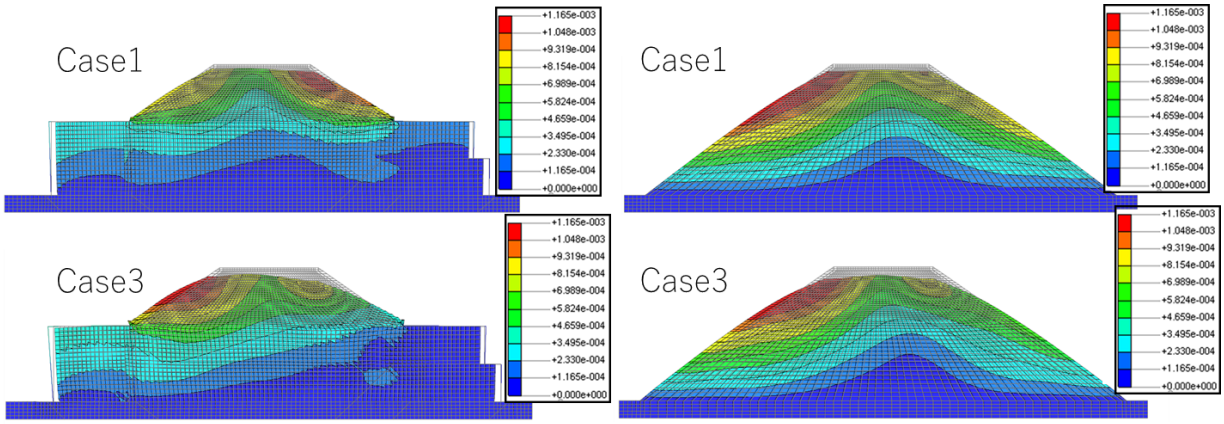

(a) Model of flexible container bag (b) Model of embankment without reinforcement

Fig. 24. Residual deformation diagram (Unit: m, deformation rate of 200 times).

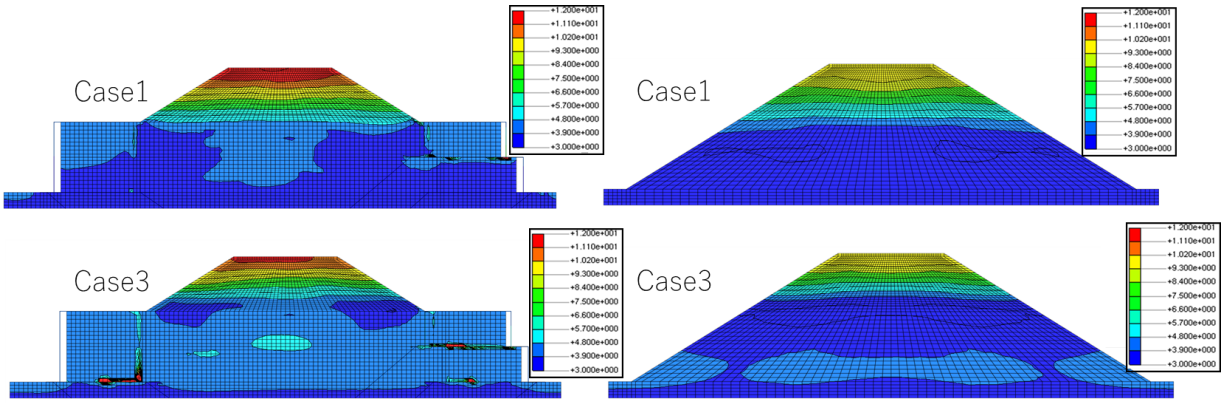

(a) Model of flexible container bag (b) Model of embankment without reinforcement

Fig. 25. Distribution diagrams of the maximum acceleration (Unit: m/s^2).

Table 5. Amplification rate of acceleration.

Case3 (376Gal)		Numerical analysis		Full-scale experiment	
Model	Location	Number of node	Amplification rate (times)	Sensor	Amplification rate (times)
One-tier model	Shoulder of slope	5209	2.92	A26	15.06
	Upper part of flexible container bag	3543	1.23	A32	4.13
Two-tier model	Shoulder of slope	5267	2.86	A28	12.56
	Upper part of flexible container bag	3603	1.19	A35	2.30
Embankment without reinforcement	Shoulder of slope	3111	2.60	—	—
		3169	2.60	—	—

little but this did not lead to a large-scale collapse.

From the results of the measurement of 3D dynamic displacement sensor, it can be seen that the horizontal displacement on the side of one-tier type was smaller than that on the side of two-tier type. As for the vertical displacement, it increased with the increase in horizontal displacement immediately after the shaking on the side of one-tier type, while in case of two-tier type, the displacement became smaller and there was also a delay in its generation.

From the results of 3D territorial laser measurement, the horizontal displacement of the top frame of compression plate of the flexible container bag of one-tier type exceeded a little compared to that of two-tier type. However, the deformation of the shoulder of slope in two-tier type was smaller.

From the results of the full-scale experiment and the numerical analysis focusing on the amplification rate at the shoulder of embankment, it can be recognized that the amplification rate of the upper part of the flexible container bag of one-tier type was larger than that of two-tier type, which seems to render the structure vulnerable at the top of the slope of embankment.

From the above comparisons, it seems that two-tier type would be slightly superior to one-tier type. However, for practical use in the future, form, size, workability, economy of embankment, etc. should be examined and experiment data should be analyzed to establish the appropriate design and method of construction.

Acknowledgements

This study is conducted as part of the joint research between the National Research Institute for Earth Science and Disaster Resilience (NIED) and Hyogo Prefecture, and the joint agreement between Hyogo Prefecture and Kobe University. A part of this study is subsidized by the Grant-in-Aid for Scientific Research of the Japan Society for the Promotion of Science (Grant-in-Aid for Scientific Research (A) (General), 19H00810 "Research on practical implementation of economic method of construction for earthquake resistance reinforcement of existing embankment using flexible container bag," Representative researcher: Satoshi Shibuya). In carrying out the experiment and summarizing the results, we received precious advice from "Committee on promotion of disaster mitigation measures using E-Defense practically" (Chairperson: Tsuneo Okada). We express our appreciation to everyone concerned.

References:

[1] Editorial committee for the report on the Hanshin-Awaji Earthquake disaster, "Report on the Hanshin-Awaji Earthquake disaster, Civil Engineering/Ground 2, Damage to Civil Engineering Structures," Japan Society of Civil Engineers, pp. 117-120, 1998 (in Japanese).

[2] The Committee on Earthquake Damage in Makinohara District of the Tomei Expressway, "Tomei Expressway Makinohara Area Earthquake Disaster Response," Road Disaster Prevention Seminar, November 2009, No.14, pp. 1-9, 2009 (in Japanese).

[3] The Committee on New Road Technology, "Economic seismic diagnosis and development of seismic reinforcement for road embankment landfilled in the valley (February, 2018) report," Ministry of Land, Infrastructure, Transport and Tourism, Chapter 1, pp. 1-4, 2019 (in Japanese).

[4] The Committee on Verification and Evaluation of 2011 Academic Recommendations, "Issues and countermeasures for ground disasters during earthquakes –Lessons learned and recommendations for the 2011 Great East Japan Earthquake–," The Japan Geotechnical Society, p. 13, 2012 (in Japanese).

[5] T. Hashimoto and K. Kawamura, "Chapter 5: Road damage," Japan Society of Civil Engineers and the Japan Geotechnical Society (Eds.), "Survey Report on the Noto Hanto Earthquake in 2007," pp. 132-215, 2007 (in Japanese).

[6] Central Nippon Expressway Company Limited, "Tomei Expressway Makinohara Area Earthquake Disaster Survey Committee Report," 2009, https://www.c-nexco.co.jp/images/press_conference/44/12797178954e004ffa764cb.pdf (in Japanese) [accessed March 27, 2020]

[7] S. Shibuya, K. Jeong, J. Baek, and K. Tani, "Aseismic reinforcement at the toe of embankment using sandbag-structure –Part 1: Basic idea–," 51st Japan National Conf. on Geotechnical Engineering, pp. 1129-1130, 2016 (in Japanese).

[8] T. Kuda, S. Shibuya, S. Kataoka, R. Tajima, Y. Moriyoshi, Y. Morigichi, and H. Nakazawa, "Enhancing aseismic stability of road embankment by reinforcing the toe with soil-bag structure – Model tests of stacking soil-bag," Geosynthetics Engineering J., Vol.32, pp. 175-182, 2017 (in Japanese with English abstract).

[9] S. Shibuya, K. Tani, S. Kataoka, and H. Nakazawa, "Aseismic Reinforcement of in-service Embankment using "Soil-bag Structure"," Geotechnical Engineering Magazine, Vol.66, No.6, Ser.No.725, pp. 28-31, 2018 (in Japanese).

[10] S. Kataoka, T. Kuda, S. Shibuya, H. Nakazawa, R. Tajima, and T.-N. Lohani, "Development of a new aseismic reinforced construction method by using soil-bag stacks at the toe section of the embankment," 16th Asian Regional Conf. on Soil Mechanics and Geotechnical Engineering, SA03-02-003, 2019.

[11] P. C. Jennings, "Periodic Response of General Yielding Structure," J. of the Enginerring Mechanics Division, Vol.90, No.2, pp. 131-166, 1964.

[12] Y. Sawada, H. Nakazawa, T. Oda, S. Kobayshi, S. Shibuya, and T. Kawabata, "Seismic Performance of Small Earth Dams with Sloping Core Zones and Geosynthetic Clay Liners by Full-Scale Shaking Table Tests," Soils and Foundations, Vol.58, No.3, pp. 519-533, 2018.

[13] D. D. Langton, "The Panda lightweight penetrometer for soil investigation and monitoring material compaction," Ground Engineering, Vol.32, No.9, pp. 33-37, 1999.

Name:
Hiroshi Nakazawa

Affiliation:
Principal Research Fellow, Earthquake Disaster Mitigation Research Division, National Research Institute for Earth Science and Disaster Resilience (NIED)

Address:
3-1 Tennodai, Tsukuba, Ibaraki 305-0006, Japan

Brief Career:

2000- Research Associate, Tokyo University of Science
2007- Project Leader, Port and Airport Research Institute
2015- Principal Research Fellow, National Research Institute for Earth Science and Disaster Resilience (NIED)

Selected Publications:

• "Experimental evaluation on earthquake-resistance of road retaining wall using gabion," J. Disaster Res., Vol.13, No.5, pp. 897-916, 2018.
• "Problems in Earthquake Resistance Evaluation of Gabion Retaining Wall Based on Shake Table Test with Full-Scale Model," J. Disaster Res., Vol.14, No.9, pp. 1154-1169, 2019.
• "Basic Study on Deformation Evaluation of Steel Wire Mesh for Rational Gabion Structure Design," EPI Int. J. of Engineering, Vol.2, No.2, pp. 109-115, 2019.

Academic Societies & Scientific Organizations:

• Japanese Geotechnical Society (JGS)
• Japan Society of Civil Engineers (JSCE)
• Japan Association for Earthquake Engineering (JAEE)
• Society of Exploration Geophysicists of Japan (SEGJ)
• Architectural Institute of Japan (AIJ)
• Geo-Risk Society (GRS)

Name:
Yohsuke Kawamata

Affiliation:
Chief Researcher, Earthquake Disaster Mitigation Research Division, National Research Institute for Earth Science and Disaster Resilience (NIED)

Address:
1501-21 Nishikameya, Mitsuda, Shijimicho, Miki, Hyogo 673-0515, Japan

Brief Career:
1998- Fudo Tetra Corporation
2001- Associated Research Fellow, Port and Airport Research Institute
2010- Associated Research Fellow, National Research Institute for Earth Science and Disaster Resilience (NIED)
2015- Chief Researcher, National Research Institute for Earth Science and Disaster Resilience (NIED)

Selected Publications:
• "Dynamic Behaviors of underground structures in E-Defense shaking experiments," Soil Dynamics and Earthquake Engineering, Vol.82, pp. 24-39, doi: 10.1016/j.soildyn.2015.11.008, 2016.
• "Large-scale Shake Table Test on Behavior of Underground Structure with the Curved Portion During an Earthquake," J. Disaster Res., Vol.12, No.5, pp. 868-881, doi: 10.20965/jdr.2017.p0868, 2017.

Academic Societies & Scientific Organizations:
• Japanese Geotechnical Society (JGS)
• Japan Society of Civil Engineers (JSCE)
• Architectural Institute of Japan (AIJ)

Name:
Satoru Shibuya

Affiliation:
Professor, Graduate School of Technology, Kobe University

Address:
1-1 Rokkodai-cho, Nada-ku, Kobe, Hyogo 657-8501, Japan

Brief Career:
1985- Research Assistant, Imperial College
1988- Research Associate, University of Tokyo
1991- Associate Professor, Hokkaido University
1996-1998 Associate Professor, Asian Institute of Technology
2003- Professor in Geotechnical Engineering, Kobe University

Selected Publications:
• "Mitigation of Disasters by Earthquakes, Tsunamis, and Rains by Means of Geosynthetic-Reinforced Soil Retaining Walls and Embankments," Transp. Infrastruct. Geotech, Vol.1, No.3-4, pp. 231-261, doi: 10.1007/s40515-014-0009-0, 2014.

Academic Societies & Scientific Organizations:
• International Society for Soil Mechanics and Geotechnical Engineering (ISSMGE)
• Japanese Geotechnical Society (JGS)
• Japan Society of Civil Engineers (JSCE)
• International Geosynthetics Society (IGS)

Name:
Shoji Kato

Affiliation:
Associate Professor, Graduate School of Technology, Kobe University

Address:
1-1 Rokkodai-cho, Nada-ku, Kobe, Hyogo 657-8501, Japan

Brief Career:
1985- Konoike Construction Co., Ltd.
1988- Technical Assistant, Kobe University
1991- Assistant Professor, Nagoya Institute of Technology
1996- Assistant Professor, Kobe University
1998- Associate Professor, Kobe University

Selected Publications:
• "Effect of suction stress on the critical state of compacted silty soils under low confining pressure," Int. J. of Geomechanics, Vol.16, Issue 6, doi: 10.1061/(ASCE)GM.1943-5622.0000665, 2016.

Academic Societies & Scientific Organizations:
• Japanese Geotechnical Society (JGS)
• Japan Society of Civil Engineers (JSCE)

Name:
Kyung-Beom Jeong

Affiliation:
Research Fellow, Graduate School of Engineering, Kobe University

Address:
1-1 Rokkodai-cho, Nada-ku, Kobe, Hyogo 657-8501, Japan

Brief Career:
2007- ESCO Consultant & Engineers Co., Ltd.
2015- Research Fellow, Kobe University

Selected Publications:
• "Seismic performance and numerical simulation of earth-fill dam with geosynthetic clay liner in shaking table test," Geotextiles and Geomembranes, Vol.48, Issue 2, pp. 190-197, doi: 10.1016/j.geotexmem.2019.11.006, 2020.

Academic Societies & Scientific Organizations:
• Japanese Geotechnical Society (JGS)
• Japan Society of Civil Engineers (JSCE)
• International Geosynthetics Society (IGS)

Name:
Jemin Baek

Affiliation:
Research Fellow, Graduate School of Engineering, Kobe University

Address:
1-1 Rokkodai-cho, Nada-ku, Kobe, Hyogo 657-8501, Japan

Brief Career:
2015- Research Fellow, Kobe University

Selected Publications:
• "Full-scale model test on the applicability of L-shaped geosynthetic drain system to Terre Armée wall against heavy rainfall," Geosynthetics Engineering J., Vol.28, pp. 353-360, doi: 10.5030/jcigsjournal.28.353, 2013.

Academic Societies & Scientific Organizations:
• Japanese Geotechnical Society (JGS)
• Japan Society of Civil Engineers (JSCE)
• International Geosynthetics Society (IGS)

Name:
Tara Nidhi Lohani

Affiliation:
Senior Technical Staff and Researcher, Kobe University

Address:
1-1 Rokkodai-cho, Nada-ku, Kobe, Hyogo 657-8501, Japan

Brief Career:
2000- Special Researcher at The University of Tokyo, National Institute of Rural Engineering, Kobe University (JSPS), and Geo-Research Institute Co., Ltd.
2013- Technical Staff and Researcher, Kobe University

Selected Publications:
• "Reviewing the 2016 Kumamoto Earthquake Damage in Mashiki Town Area by using Microtremor Measurements," Int. J. of Safety and Security Eng., Vol.7, No.4, pp. 577-584, doi: 10.2495/SAFE-V7-N4-577-584, 2016.

Academic Societies & Scientific Organizations:
• Japanese Geotechnical Society (JGS)
• Nepal Geotechnical Society (NGS)
• Nepal Geological Society (NGS)
• Nepal Engineers' Association (NEA)

Name:
Akihira Morita

Affiliation:
Assistant Section Chief, Hyogo Prefecture

Address:
5-10-1 Shimoyamate Street, Kobe, Hyogo 650-8567, Japan

Brief Career:
2005- Private Company
2016- Hyogo Prefecture

Name:
Osamu Takemoto

Affiliation:
Senior Manager, Hyogo Prefecture

Address:
5-10-1 Shimoyamate Street, Kobe, Hyogo 650-8567, Japan

Brief Career:
1997- Hyogo Prefecture

Name:
Yoshitaka Moriguchi

Affiliation:
Group Leader, Hyogo Prefecture

Address:
5-10-1 Shimoyamate Street, Kobe, Hyogo 650-8567, Japan

Brief Career:
1994- Hyogo Prefecture